

Contents lists available at [SciVerse ScienceDirect](http://www.sciencedirect.com)

Chemical Engineering Journal

journal homepage: www.elsevier.com/locate/cejChemical
Engineering
Journal

Paper-like composites of cellulose acetate–organo-montmorillonite for removal of hazardous anionic dye in water

Chun-Hui Zhou^{a,*}, Di Zhang^a, Dong-Shen Tong^a, Lin-Mei Wu^a, Wei-Hua Yu^a, Suryadi Ismadji^b^a Research Group for Advanced Materials & Sustainable Catalysis (AMSC), Breeding Base of State Key Laboratory of Green Chemistry Synthesis Technology, College of Chemical Engineering and Materials Science, Zhejiang University of Technology, Hangzhou 310032, China^b Department of Chemical Engineering, Widya Mandala Surabaya Catholic University, Kalijudan 37, Surabaya 60114, Indonesia

H I G H L I G H T S

- ▶ Paper-like cellulose acetate/organo-montmorillonite composites were prepared.
- ▶ Good dispersion of organo-montmorillonite and cellulose acetate was achieved in acetone.
- ▶ The adsorption capacity of the composites for Acid Scarlet G dye reached 85.7 mg g⁻¹.
- ▶ The Lagergren's first-order equation was found to be suited for the adsorption kinetics.
- ▶ The adsorption was endothermic and the isotherm fitted into the Langmuir equation.

A R T I C L E I N F O

Article history:

Received 23 May 2012

Received in revised form 24 July 2012

Accepted 24 July 2012

Available online 2 August 2012

Keywords:

Montmorillonite

Cellulose acetate

Inorganic–organic composite

Adsorption

Anionic dye

Wastewater

A B S T R A C T

The shaped solid composites of biopolymers and clay minerals have great potential in the efficient removal of hazardous pollutants from wastewater. Here novel paper-like cellulose acetate/organo-montmorillonite (CA/OMMT) composites were prepared from cellulose acetate (CA) and organo-montmorillonite (OMMT). CA and OMMT were dispersed in acetone, followed by evaporation and drying, thereby leading to paper-like solid CA/OMMT composites. The resulting composite samples were characterized by using X-ray diffraction, Fourier transform infrared spectroscopy, scanning electron microscopy, and thermal gravimetric analyses. The adsorption of Acid Scarlet G (ASG) anionic dye in aqueous solution onto the CA/OMMT composites was tested by varying the pH value of the dye solution, the temperature and time, and the initial dye concentration. The organic modification of montmorillonite facilitated the intercalation of the motifs of CA molecules into the interlayer space of OMMT. There was the intermolecular and intramolecular linkage among CA molecules and OMMT platelets. Dependent on the ratio of CA to OMMT, the composites had a dense or a macroporous paper-like structure. The adsorption capacity of the composites increased with the decrease of the ratio of CA to OMMT and the pH value of the dye solution. The adsorption rate was enhanced with the increase of the temperature. The adsorption was a kinetically controlled, spontaneous and endothermic process. The Lagergren's first-order equation was found to be suited for the adsorption kinetics of ASG onto the CA/OMMT composite. The adsorption isotherm of ASG onto CA/OMMT composites fitted into the Langmuir equation.

© 2012 Elsevier B.V. All rights reserved.

1. Introduction

Cationic layered clay minerals, such as montmorillonite, saponite and hectorite, feature peculiar ion exchange, swelling, and large surface areas in aqueous system. Accordingly, they have high reactivity and adsorption [1,2]. The modification and shaping of these clay minerals into functional materials has received much attention over the past decades because they are useful in many

fields, including adsorption and separation [3]. Many studies have revealed that the naturally-occurring clay minerals in their pristine form can act as adsorbents [4]. They substantially get involved in the adsorption, fixation and transformation of organic matter in nature [5]. However, they usually need modifying and shaping for laboratory and industrial purposes [6]. Noticeably, the thickness of a single layer of clay minerals is around one nanometer and, dependent on the type and amount of the exchangeable ions or the guest molecules in their interlayer space, the gallery height can be altered from several angstroms to a few nanometers. Such nanometer-scaled layered structures of clay minerals allows a great many approaches to be applied to tailor their physical and

* Corresponding author. Tel.: +86 571 88320062.

E-mail address: chc.zhou@yahoo.com.cn (C.-H. Zhou).

chemical properties on their surface, in their framework, and within their interlayer space [7,8].

For the adsorption of organic pollutants, the modification of clay minerals is usually made through the ion exchange reaction and intercalation by guest organic species [9]. Organo-montmorillonite clays (OMMT), for example, can be obtained through the ion exchange reaction between cations in the interlayer space of montmorillonite clay minerals and organic cations [10]. In this way, the organophobic interlayer space of montmorillonite clay minerals are converted to organophilic one. By contrast with the pristine montmorillonite, the resultant OMMT materials display a much higher rate and capacity in the adsorption of organic ions and molecules [11,12]. Hence, so far OMMT materials as a class of adsorbents have been widely tested in the removal of organic pollutants from wastewater [13].

Adsorptive materials are particularly attractive in the removal of the colored, toxic organic compound from wastewater in dye industry [14,15]. Typically, the water containing Acid Scarlet G (ASG), a frequently used dye in industry, is not only harmful to the aquatic organisms and plants, but also is hazardous to human beings. Activated carbon [16,17], chitosan modified montmorillonite [18], cross-linked chitosan film [19], and amine functionalized titania/silica nano-hybrid [20] have been tested as adsorbents for the removal of ASG from wastewater. In many cases, the practical applications of these materials are limited either by the low adsorption capacity or the difficulty of separation. Owing to these defects, many of them are rarely put into practical use. Therefore, the development of new materials is still needed. Previously, the powder OMMT was found to be able to adsorb ASG in aqueous solution [21]. However, the use of OMMT in the powder form for the treatment of wastewater on an industrial scale leads to great difficulty in separating them from water after the adsorption. In this context, a solution is to shape OMMT into a type of easily operable bulky material.

Noticeably, the composites of organic polymers and inorganic clay minerals are a class of bulky and moldable solid materials. These composites can be shaped into membranes and films [5,22]. Recently, with the dwindling of fossil fuels, which are the basic feedstock for the production of many of present polymers, biopolymers and their composites with layered clay minerals have captured particular attention [23]. Clearly, it is of great significance to develop adsorptive composites from biopolymers and layered clay minerals for the removal of organic hazardous pollutants in water. First of all, both biopolymers and clay minerals are non-toxic and nonhazardous to the environment, animals and human beings. In addition, biopolymers are degradable in the natural system [24]. Among various biopolymers, cellulose is the most abundant one on earth [25]. Moreover, it can be converted into various derivatives through chemical reactions. Recently, several studies described a new type of composites prepared from cellulose or cellulose-derived molecules and clay minerals under judiciously chosen conditions [26,27]. Remarkably, the composites of clay minerals and cellulose acetate (CA) were found to possess the peculiar physical and chemical properties [28]. Nevertheless, the clay minerals were used as fillers for those composites and the quantity of clay minerals in them was usually less than 5 wt.% [29]. Therefore, those composites are not suitable to be used as adsorbents because of the lack of adsorptive properties [30]. It is still desired to produce a kind of composites which not only have proper adsorption capacity but also can be easily handled in wastewater treatment.

Here attempts were made at the preparation of novel paper-like composites from cellulose acetate and organo-montmorillonite clays (CA/OMMT). The adsorption of ASG anionic dye as a model pollutant in aqueous solution onto the resulting paper-like CA/OMMT composites was then evaluated. The effects of the ratio of CA to OMMT, the pH value of the dye solution, adsorption temperature,

adsorption time and the initial concentration of the dye on the adsorption of the CA/OMMT composites were explored. Finally, the adsorption kinetic and thermodynamic models were discussed. It is expected that, with the much addition of clay minerals in them, such paper-like composites can be used as new materials to adsorb the hazardous organic ions and molecules in water. In particular, because the composites are made into the insoluble paper-like form, the transportation, use and separation of them after adsorption in the treatment of wastewater will become much easy and economic.

2. Experimental

2.1. Materials and chemicals

Raw montmorillonite minerals (Ca-montmorillonite) were provided by Renheng Co., Ltd., China. The powders of the montmorillonite with the sizes less than 100 mesh were used. Cetyl trimethylammonium bromide (CTAB) [$C_{16}H_{33}(CH_3)_3NBr$] was purchased from Shanghai Bio Science & Technology, Co., Ltd., China, with a purity of 98%. Acid Scarlet G (ASG) (Azophloxine, $C_{18}H_{13}N_3Na_2O_8S_2$) (Fig. 1A) was a commercially available textile dye and used without further purification. Cellulose acetate (CA) (Fig. 1B) was a commercially available chemical with average acetyl content of 39.8 wt.% and a degree of substitution of 2.45. The average molecular weight (Mw) of the CA was measured by gel permeation chromatography (GPC) on a Waters 510 series system with polystyrene standards for column calibration and the Mw value obtained was 50,000. All other chemicals and reagents were of analytical grade and were used without further purification.

2.2. Preparation of Na-rich montmorillonite

Na-rich montmorillonite (MMT) was obtained through the ion exchange. 10.0 g of montmorillonite mineral powders were dispersed in 500 mL of distilled water. The mixture was stirred for 1 h with a mechanical stirrer at 300 rpm to form a suspension. Then 0.8 g of NaOH was added into the suspension and the suspension was mechanically stirred at 200 rpm at room temperature for 12 h. The slurry was centrifuged at 4500 rpm for 30 min. The solid was transferred to an evaporating dish and dried in an oven at 105 °C in air for 24 h. After that, the solid was ground and sifted through a sieve of 100 mesh size to yield a powder sample, which was labeled as Na-rich MMT. The cation exchange capacity (CEC) of the obtained Na-rich MMT was determined by the ammonium acetate method and it was 87 mmol/100 g MMT.

2.3. Preparation of organo-montmorillonite

The organically modified MMT (OMMT) was prepared by the following procedure. The surfactant CTAB [$C_{16}H_{33}(CH_3)_3NBr$], the molar amount of which was two times the CEC of 4.0 g of Na-rich MMT, was first dissolved in 100 mL of distilled water. Next, 4.0 g of Na-rich MMT was slowly added into it. The mixture was stirred at 60 °C for 12 h, followed by centrifugation at 4500 rpm for 30 min. Then, the solid was washed several times with distilled water until no bromide ion was detected by using an aqueous $AgNO_3$ solution (0.1 M). After the solid was dried in an oven at 105 °C, it was ground, sifted through a 100 mesh size sieve to yield a powder OMMT sample.

2.4. Preparation of paper-like cellulose acetate-organomontmorillonite composites

0.12 g of OMMT powder was dispersed in 1.5 mL of acetone with magnetic stirring. The suspension was then treated by ultrasonification for 1 h, thereby leading to a good dispersion of OMMT

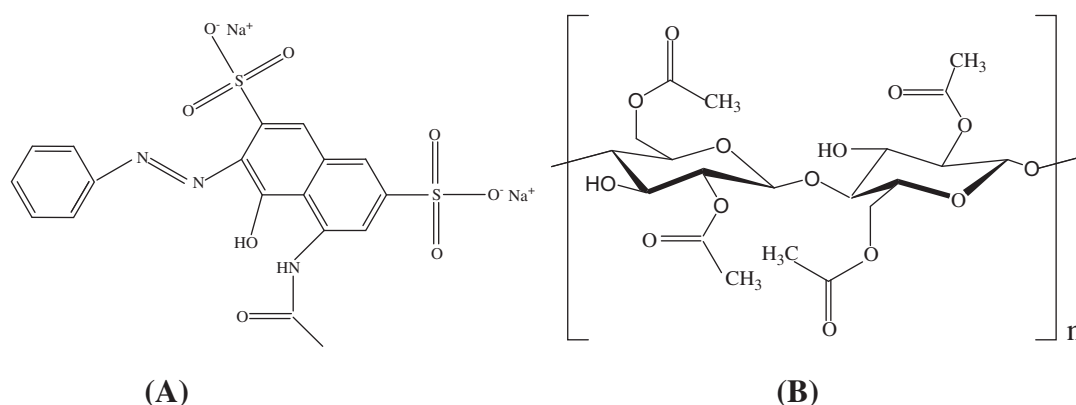


Fig. 1. (A) The molecular structure of Acid Scarlet G [ASG, 2,7-naphthalenedisulfonic acid, 5-(acetylamino)-4-hydroxy-3-(phenylazo)-, disodium salt]. (B) The structure of cellulose acetate.

in acetone. A solution of 0.08 g of CA in 4.7 mL of acetone was made and then was added to the suspension of OMMT in acetone. The composition of mixture is kept at a weight ratio of CA:OMMT:acetone of 4/6/490. The mixture was stirred at room temperature for 24 h. Then the mixture was poured into a glass Petri dish to allow the solvent to evaporate gradually under ambient condition. After that, the dried paper-like sample was peeled off and was named as CA/OMMT_{60%}. By using the similar procedure, a series of CA/OMMT composite samples were made by varying the content of OMMT so that the OMMT in the resultant CA/OMMT composites took up a percentage of 10 wt.%, 20 wt.%, and 40 wt.%, respectively. The samples were labeled as CA/OMMT_{10%}, CA/OMMT_{20%}, and CA/OMMT_{40%}, respectively.

2.5. Characterization of Na-rich MMT, OMMT and paper-like CA/OMMT composites

The X-ray diffraction (XRD) patterns of the powder samples of Na-rich MMT and OMMT was detected on a Thermo ARL SCINTAG X'TRA diffractometer equipped with CuK α radiation at a wavelength of 1.54056 Å. The reflections were recorded in the 2θ range of 2° to 40° at a scanning rate of 0.1°/s. The basal spacing of MMT (d_{001}) was calculated through the Bragg's equation ($n\lambda = 2d\sin\theta$). The XRD patterns of the CA/OMMT composites were recorded in the 2θ range of 2–12° by using the as-made paper-like samples. Different from the use of the powders of Na-rich montmorillonite and OMMT samples, the samples of paper-like CA/OMMT composites were directly put on a glass plate for the XRD detection.

The Fourier transform infrared spectra (FTIR) of MMT and OMMT samples were recorded on a Nicolet AVATAR-370 spectrometer. Prior to the use, each sample was dried at 110 °C. It was then mixed with KBr and the resulting mixture was pressed into a wafer. Under ambient conditions, the spectra of the wafer samples were measured at averaging 32 scans/s at 0.1 cm⁻¹ resolution in the wavenumber ranging from 4000 to 400 cm⁻¹.

Micrographs of the paper-like composite samples were taken on a scanning electron microscope (SEM) (Hitachi-4700, JEOL). Each sample was fixed on an aluminum stub and coated with gold.

Thermogravimetric analysis (TGA) of the paper-like composite samples was performed on a Shimadzu TG 60 thermal analyzer. For each test, about 10–15 mg of the sample was loaded into the alumina crucible and was then heated from room temperature to 900 °C at a programmed rate of 10 °C/min in a flow of nitrogen.

2.6. Adsorption experiments

For the investigation of the effects of the composition of each paper-like CA/OMMT composite on its adsorption of ASG, 100 ml

of aqueous ASG solution with an initial concentration of 50 mg L⁻¹ and a pH value of 5.5 was used in each run. To such a dye solution, 0.05 g CA/OMMT composites were added as the adsorbents. The solution with CA/OMMT in it was shaken at 120 rpm at 20 °C for 12 h. After that, the paper-like CA/OMMT was taken out from the solution. Then the solution was used for quantitative analyses. The concentration of ASG in solution was measured on ultraviolet (UV) spectrophotometer (Mode-722, China) at a specific wavelength for ASG (510 nm).

The amount of the dye adsorbed onto CA/OMMT composite was calculated through the following equation:

$$q_e = \frac{(C_0 - C_e)V}{m} \quad (1)$$

where q_e is the amount of adsorbed dye (mg g⁻¹) at equilibrium, C_0 is the initial concentration of ASG in solution (mg L⁻¹), C_e is the equilibrium concentration of ASG in solution (mg L⁻¹), m is the mass of adsorbent used (g) and V is the volume of ASG solution (L). The possible loss of trace ASG caused by volatilization, sorption to the glassware and degradation was ignored.

The sample of CA/OMMT_{60%} composites, which comparatively showed the best adsorption capacity among a series of CA/OMMT samples, was selected and used for experiments on the adsorption kinetics and isotherms. The experiments were conducted by using a batch equilibrium technique. The measurement of the effects of pH value of the solution on the adsorption were carried out by using 100 ml of 50 mg L⁻¹ dye solution with 0.05 g of CA/OMMT_{60%} samples for 12 h. The pH of the solution was adjusted in the range of 1–10 through adding 1 mol/L HCl or NaOH solution in it. The optimal pH value was determined and used throughout other adsorption experiments, which were conducted at various time intervals, the initial concentrations (50, 75 and 100 mg L⁻¹) and temperatures (20, 40 and 60 °C) in order to determine the adsorption equilibrium time and the maximum removal of dye.

3. Results and discussion

3.1. Characterization of OMMT

According to the XRD patterns of the powder samples of Na-rich montmorillonite and OMMT (Fig. 2), the basal spacing of Na-rich montmorillonite and OMMT, namely d_{001} -value, is 12.6 and 22.3 Å, respectively. The interlayer space was increased by 9.7 Å after the ion exchange between Na⁺ cations and cetyl trimethylammonium cation (CTA⁺, [C₁₆H₃₃(CH₃)₃N]⁺) cations. The thickness of a single MMT layer is 9.6 Å, and the height of CTA⁺ with a monolayer arrangement is 4.6 Å [21,31]. Clearly, the increase of gallery height of the resulting OMMT materials was due to the intercalation of

bulky organic cations. Moreover, it suggested that the intercalated cationic surfactants in the interlayer of montmorillonite was present in a form of an oblique triple-layer arrangement, thereby giving a thickness of about 12.7 Å. The modified montmorillonite with an organic species in the interlayer space exhibited hydrophobicity. Consequently, in the experiments OMMT showed a good compatibility with the organic acetone and it was well dispersed in acetone. The use of acetone was also conducive to the dissolution of CA. Hence, the organic modification of montmorillonite enabled the good dispersion and mixing of OMMT and CA in acetone. All these were favorable to the formation of paper-like CA/OMMT composites after the evaporation of acetone.

The formation of OMMT was further evidenced by the FTIR spectra of Ca-rich montmorillonite, Na-rich montmorillonite and OMMT (Fig. 3). The absorbance bands at 3630, 3440 and 1640 cm^{-1} are characteristic of montmorillonite, arising from the stretching vibration of O–H groups, the stretching vibration and bending vibration of water molecules for the hydration in the lattice of montmorillonite, respectively [32]. The band at 3230 cm^{-1} is ascribed to hydrogen bonds among water molecules in the interlayer of the montmorillonite [33]. The band at about 1040 cm^{-1} is ascribed to the stretching vibration of the Si–O bonds, and the bands at 521 and 466 cm^{-1} are attributed to the stretching vibration and bending vibration of Si–O–Al bonds, respectively. After the ion exchange between Na^+ cations and CTA^+ [$\text{C}_{16}\text{H}_{33}(\text{CH}_3)_3\text{N}^+$] cations, the resulting OMMT appeared to have all these typical bands of Na-montmorillonite (Fig. 3A and B). This suggested that the layered structure of the montmorillonite remained and there was only the intercalation of organic species into the interlayer space of montmorillonite. As a result, the extra bands at 2850 and 2920 cm^{-1} were clearly observed after organic modification (Fig. 3B). These bands were attributed to the symmetric stretching vibration of $-\text{CH}_2$ groups and asymmetric stretching vibration of C–H bonds [34]. These partly verified the intercalation of CTA^+ ions into the interlayer of montmorillonite, in good agreement with XRD detection (Fig. 2).

3.2. XRD analysis of CA/OMMT composites

As illustrated in Fig. 4, the XRD patterns of the pure CA and the series of CA/OMMT composites appeared different. Compared with the basal reflection of the OMMT sample at $2\theta = 3.95^\circ$ (Fig. 2B), for all the CA/OMMT composites, the specific 001 reflections from the montmorillonite in CA/OMMT composites were all shifted toward the lower 2θ angle regions at around 2.89° . These were attributed

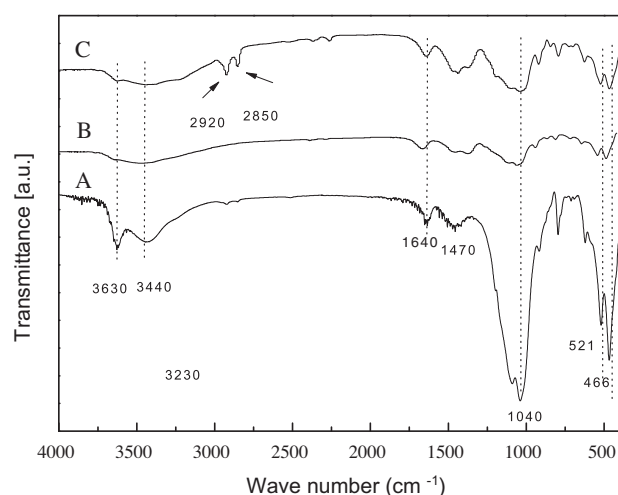


Fig. 3. FTIR spectra of (A) Ca-rich montmorillonite, (B) Na-rich montmorillonite and (C) OMMT.

to the occurrence of the further swelling of the OMMT, caused by the insertion of part of the polymer chains into their interlayer space. It meant that there was the interaction between the chains of CA polymer and OMMT, leading to the formation of paper-like CA/OMMT composites. Thus the 001 reflection of the CA/OMMT composites was shifted to the lower 2θ angle, compared with that of OMMT [35].

Moreover, the 001 reflection became increasingly sharp with the increase of the OMMT content in the CA/OMMT composites. When the OMMT content was increased to an amount of more than 20 wt.% of the composite, there were an extra reflection at around $2\theta = 5.49^\circ$ (Fig. 4D and E). It suggested that, dependent on the OMMT content, certain platelets of the OMMT were not intercalated by CA. This is reasonable to consider that dispersion of OMMT in acetone is better at a lower OMMT content than that at a higher OMMT content. Nevertheless, the 001 reflection was able to be clearly detected for all CA/OMMT composite, indicating that the substantial exfoliation of the OMMT layers did not occur when they interacted with CA molecules [36,37]. Provided that the platelets of OMMT in the resulting composites were present in a thorough exfoliated form, the 001 reflection of the MMT clay mineral would completely disappear in the XRD patterns [30,38]. However, when the concentration of OMMT used during preparation was

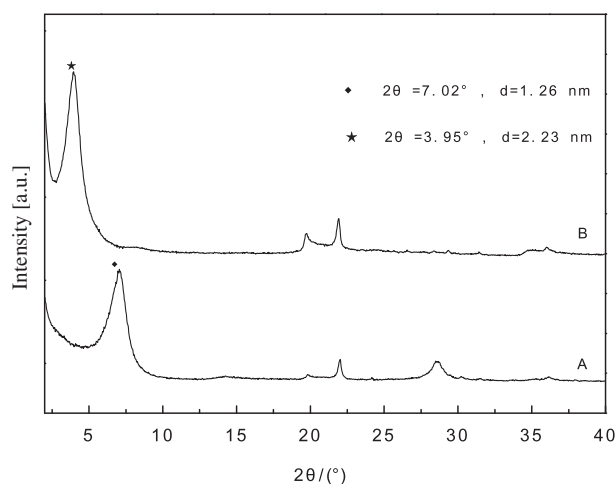


Fig. 2. XRD patterns of (A) Na-rich montmorillonite and (B) OMMT.

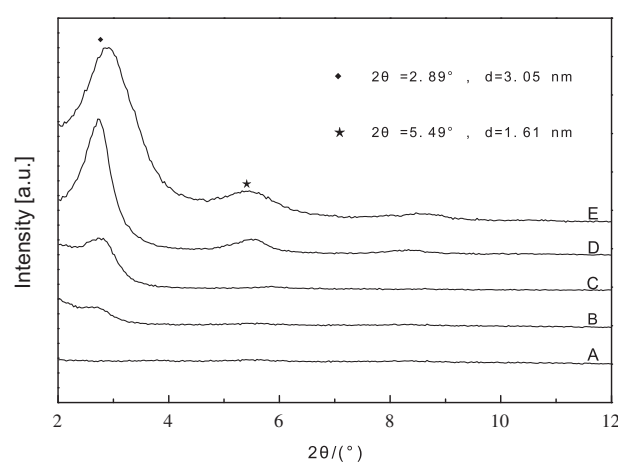


Fig. 4. XRD patterns of (A) CA, (B) CA/OMMT_{10%}, (C) CA/OMMT_{20%}, (D) CA/OMMT_{40%}, and (E) CA/OMMT_{60%}.

lower than 20 wt.%, part exfoliation of OMMT platelets was observed from the XRD patterns. This was because the more dilute the suspension of OMMT in acetone was, the more easily the OMMT was delaminated. Noticeably, when pristine Na-montmorillonite was used for preparing CA/MMT composites, by using similar preparation procedures, only a powder mixture of CA and montmorillonite was yielded. This reflected that the organic modification of montmorillonite was necessary for the formation of paper-like structure from the CA and the OMMT.

3.3. SEM analysis of paper-like CA/OMMT composites

The paper-like samples of CA and paper-like CA/OMMT composites containing 10 wt.%, 20 wt.%, 40 wt.% and 60 wt.% of OMMT were respectively observed on a field emission scanning electron microscope (Fig. 5). A smooth, uniform and macrovoid-free structure was observed for the sample of pure CA polymer, which was dispersed in acetone and then formed a solid paper-like sample after the evaporation of acetone (Fig. 5a). Though all CA/OMMT composite samples were also obtained in the paper-like shape, their morphology were found to be different, as seen from the SEM micrographs. Moreover, dependent on the OMMT contents, the structures of CA/OMMT composites varied, particularly in view of the dispersion of clay particles in them. As to the composite samples with the low content of OMMT (Fig. 5b and c), the platelets of clay mineral were uniformly dispersed within the composites. The well-dispersed platelets of OMMT were favorable to form dense structures, as shown by the observation focused on an area by further magnification (Inset micrographs). It showed that there was dense cross-linking between CA molecules and OMMT platelets and OMMT platelets were wrapped by small CA patches.

When the content of OMMT reached up to 40 wt.%, remarkable macrovoids were observed (Fig. 5d). It could be attributed to the loose cross-linking between CA molecules and OMMT platelets. When the amount of OMMT was further increased to 60 wt.%, as shown in Fig. 5e, macroporous structures was also formed. Compared with CA/OMMT_{40%}, there was difference in morphology for CA/OMMT_{60%} possibly because OMMT clay particles were more easily to form some agglomerates at higher contents. Therefore, from the differences of the morphology of the series of samples observed by the SEM, it could be deduced that there were several interactions in the CA/OMMT composites: cross-linking reactions between OMMT and CA, intermolecularly and intramolecularly; aggregations of clay platelets and part of intercalation of CA in the interlayers of OMMT. In the CA/MMT composites with low contents of OMMT, exfoliated structures were more prevalent than intercalated structures, whereas in the CA/MMT composites with high contents of OMMT macroporous structures were favorable to form.

3.4. TGA analysis of paper-like CA/OMMT composites

Thermal gravimetric analysis of the samples of Na-MMT, OMMT and CA are shown in Fig. 6a. As for the Na-MMT sample, three distinct stages of weight loss in the range of 20–120 °C, 150–440 °C, and 450–700 °C were observed. The first stage was due to the physical adsorbed water, which has a good mobility and is easy to be removed upon heating, and the weight loss was around 8.9 wt.% (Fig. 6a-A). The second stage of weight loss was due to the removal of water by the dehydration of the exchangeable cations upon heating. It was dependent on the amounts of hydrated cations in the interlayer space. This weight loss was around

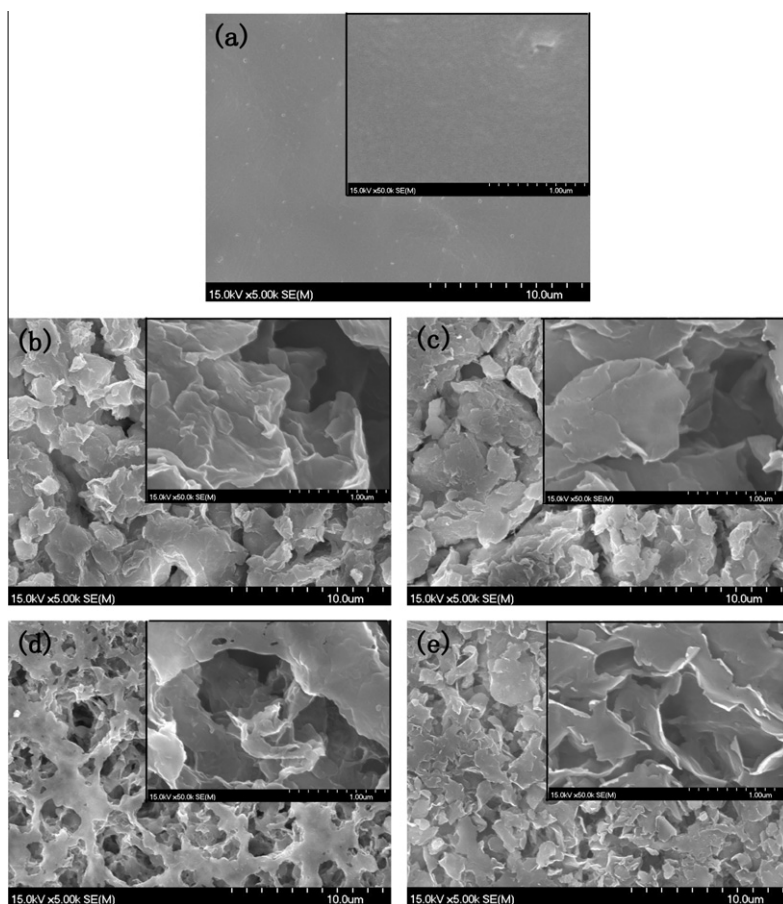


Fig. 5. SEM micrographs of CA and CA/OMMT composites.

4.8 wt.%. At higher temperatures, the dehydroxylation in the lattice of montmorillonite occurred. As to the OMMT sample (Fig. 6a-B), there was less adsorbed water on the surface because of the surface of montmorillonite had been turned from the hydrophilic into the hydrophobic. Moreover, in the range of 220–440 °C, the weight loss for the organic surfactant reached 22.7 wt.%, owing to the decomposition of the surfactant species [39]. The thermal degradation of CA involved at least three stages [40]. The first was the removal of physically bound water at the range of 30–260 °C. The second was the unzipping of the cellulose chains and then their primary decomposition to dehydrated and volatile compounds, which occurred at 300–400 °C. The third was the deep decomposition of the dehydrated product to biochar and gases at temperatures higher than 450 °C (Fig. 6a-C). Substantial weight loss of around 50.5 wt.% took place at the range of 300–450 °C. Clearly, this was caused by the degradation and the decomposition of CA [41].

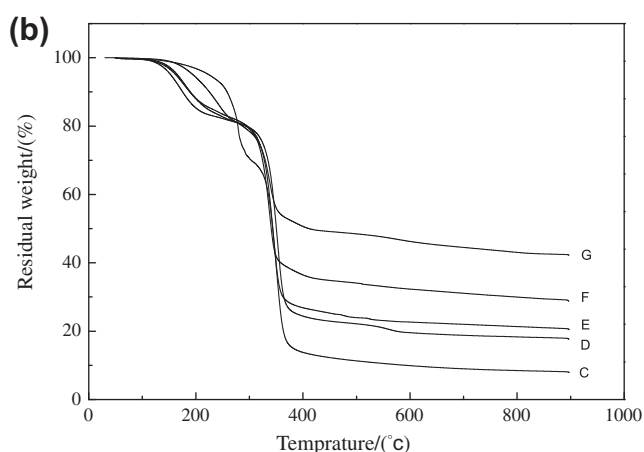
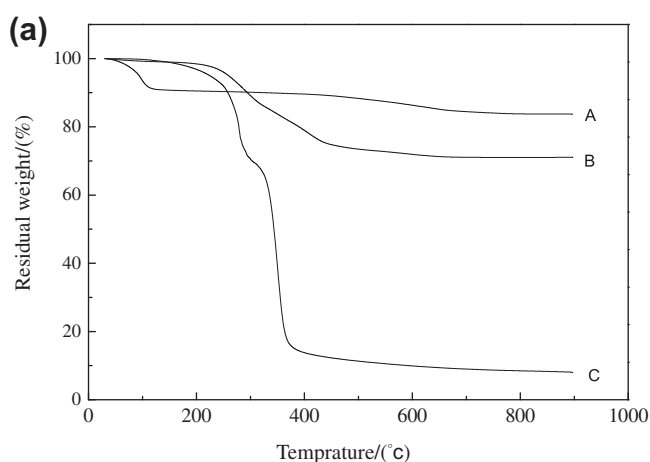
As demonstrated in Fig. 6b, the thermogravimetric curves of weight loss of paper-like CA/OMMT composites give a combined characteristic of CA and OMMT, thereby proving the formation of the composites. Typically, there are three stages of weight losses at the temperature range of 70–260 °C, 320–400 °C, and after

400 °C. The first weight loss at 70–260 °C was about 20 wt.% for all CA/OMMT composite samples. There was minor difference mainly because of the difference in the contents of OMMT in these composites, which led to different capacity of water retention on the surface of CA/OMMT composites. When the contents of OMMT was increased from 10 wt.% to 60 wt.%, for all composites samples the weight loss between 220 and 260 °C remained at around 8.0 wt.%, but then the different, rapid weight loss was detected in the range of 320–400 °C, as the weight loss came from both the OMMT and the CA. Comparatively, No obvious weight loss was observed for pure Na-MMT at these temperatures. Namely, this weight loss of CA/OMMT composites could be attributed to the structure degradation of CA and the decomposition of surfactant upon heating at high temperatures. As such, the weight loss from the decomposition and the removal of organic species on the CA/OMMT_{10%}, CA/OMMT_{20%}, CA/OMMT_{40%} and CA/OMMT_{60%} were 42.2 wt.%, 28.8 wt.%, 20.4 wt.%, and 17.6 wt.%, respectively. These values were in good agreement with the order of the ratio of CA/OMMT used during sample preparation.

3.5. Effects of the ratio of CA/OMMT and pH value on adsorption

For investigating the influence of the ratio of CA to OMMT on the adsorption of ASG onto CA/OMMT composites (Fig. 7), a series of experiments were conducted with the addition of 0.05 g of Na-rich MMT, OMMT, CA/OMMT_{10%}, CA/OMMT_{20%}, CA/OMMT_{40%}, and CA/OMMT_{60%} into a dye solution, respectively. For each run, 100 ml of 50 mg L⁻¹ dye solution at the pH of 5.5 at 20 °C and the adsorption time 12 h was used. When the content of OMMT in the CA/OMMT composites was increased from 10 wt.% to 60 wt.%, the adsorption capacities of CA/OMMT increased in the order of 3.1, 21.2, 39.1 and 85.7 mg g⁻¹. The results revealed that OMMT played a leading role in adsorption. This was also verified by the adsorption capacities of the pure powder OMMT sample, which reached 94.6 mg g⁻¹. Obviously, OMMT powder was hard to be separated because after use it became sludge. Instead, paper-like appears in a bulky form could be taken out from the water easily.

According to the adsorption capacity, the paper-like CA/OMMT_{60%} composites were then chosen for a series of studies later on. For probing the effect of the pH value of dye solution, each experiment was carried out by using 100 ml of 50 mg L⁻¹ dye solution with 0.05 g of CA/OMMT_{60%} in it for 12 h. The pH of the solution was respectively adjusted in the range of 1–10 through adding 1 mol/L HCl or NaOH solution into it at a required amount. The



(a) A. MMT, B. OMMT, C. CA;

(b) D. CA/OMMT_{10%}, E. CA/OMMT_{20%}, F. CA/OMMT_{40%}, G. CA/OMMT_{60%}

Fig. 6. TGA curves of MMT, OMMT, CA and CA/OMMT composites. (a) A. MMT, B. OMMT, C. CA, (b) D. CA/OMMT_{10%}, E. CA/OMMT_{20%}, F. CA/OMMT_{40%}, G. CA/OMMT_{60%}.

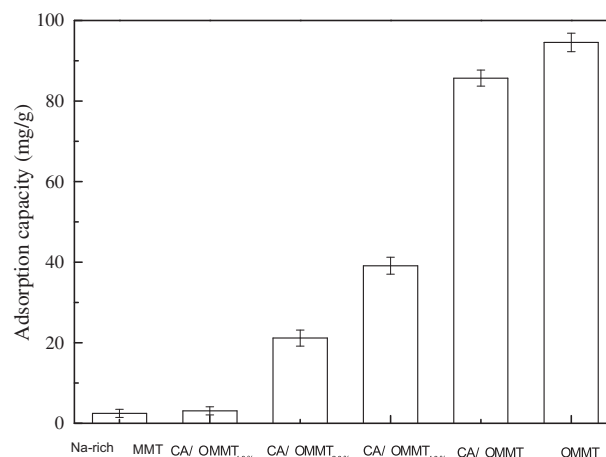


Fig. 7. Effect of the composition of Na-rich MMT, OMMT and CA/OMMT composites on the adsorption of ASG onto them.

adsorption was found to be dependent on the pH value of the dye solution (Fig. 8). As seen from the molecular structure of ASG (Fig. 1A) and the structural features of montmorillonite, the pH value of the dye solution can affect both the surface charge of the adsorbent and the degree of ionization of the adsorbate ASG. In particular, the degree of ionization of ASG directly related to its pKa values. According to the measurement made by Biçer and Arat [42], the pKa values of ASG were 7.5 (azonium group, pKa1) and 10.0 (naphtholic group, pKa2), respectively. At pH = 1, the adsorption capacity of the CA/OMMT_{60%} composites reached the maximum of 95.1 mg g⁻¹, whereas at pH = 9, the adsorption capacity gave the minimum of 61.7 mg g⁻¹. Such a gap of 33.4 mg g⁻¹ was attributed to the strong electrostatic interaction between the [C₁₆H₃₃(CH₃)₃N]⁺ in OMMT and dye anions and the ionization of azonium group took priority at low pH [43]. When the pH value of the dye solution was raised from 1 to 10, the ionization of naphtholic group made the negative charge on the ASG in the solution increase. Also, the adsorbent surface, namely montmorillonite layer surfaces, appeared negatively charged. As a result, a decreased adsorption at high pH values was observed. This was due to the abundance of OH⁻ ions in solution, leading to the ionic repulsion between the negatively charged surface and the anionic dye molecules [44].

3.6. Effects of initial dye concentration, contact time and temperature on adsorption

The initial concentrations of aqueous ASG solution in the range of 25–125 mg dm⁻³ were used to probe their influences on the rate of adsorption of the paper-like CA/OMMT_{60%} composites at pH = 1 and at 20, 40 and 60 °C, respectively. As depicted in Fig. 9, when the initial concentration of the dye was increased from 25 and 125 mg dm⁻³, the adsorption capacity of the CA/OMMT_{60%} composites increased from 48.4 to 165.2 mg g⁻¹ at 20 °C, from 49.3 to 177.6 mg g⁻¹ at 40 °C, and from 50.0 to 193.4 mg g⁻¹ at 60 °C, respectively. These indicated that the initial concentration of dye had a remarkable effect on the adsorption of ASG onto the CA/OMMT_{60%} composites. Clearly, the increase of the temperature was favorable to the adsorption.

The effect of contact time on the amount of ASG adsorbed onto the CA/OMMT_{60%} composites at various temperatures (Fig. 9) was investigated by varying initial concentration of dye from 25 to 125 mg dm⁻³, respectively. When the contact time was increased, the amount of adsorption was increased slightly. By contrast, the rate of the adsorption of ASG onto the CA/OMMT_{60%} composites was greatly affected by the temperature. Nevertheless, the time

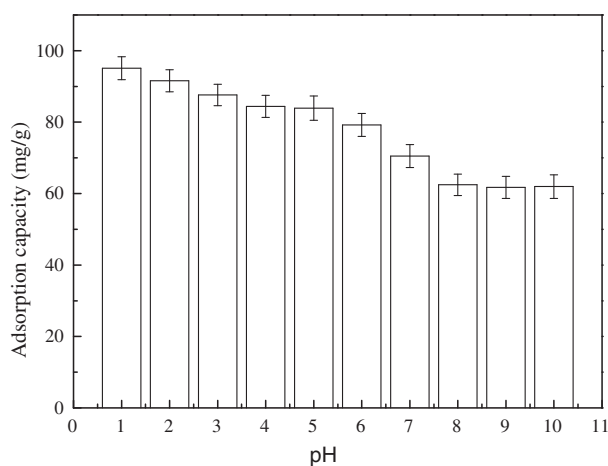


Fig. 8. Influence of the pH values on adsorption capacity of CA/OMMT_{60%} for ASG.

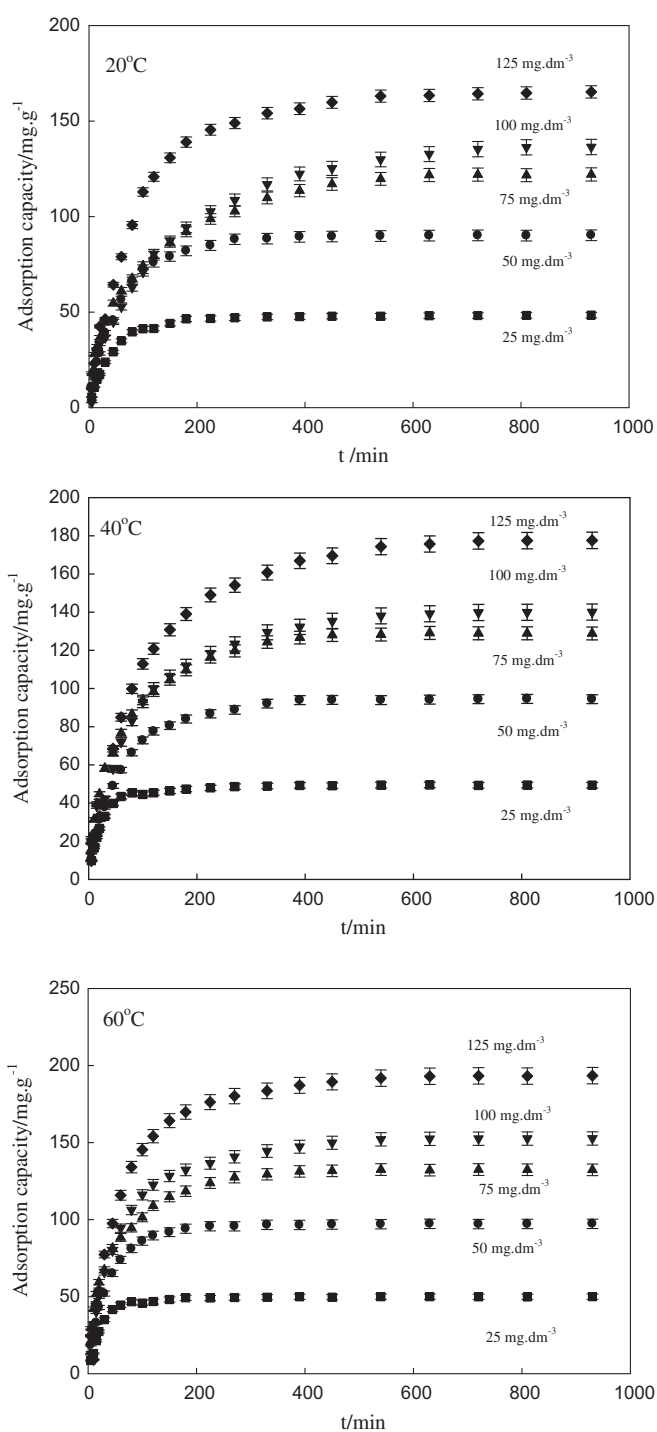


Fig. 9. Effect of contact time for the adsorption of ASG onto CA/OMMT_{60%} at temperature: (a) 20 °C, (b) 40 °C and (c) 60 °C.

to reach the equilibrium of adsorption depended on the initial concentration of dye and temperature. At 20 °C, the maximum capacities of the adsorption of ASG onto the CA/OMMT_{60%} composites were achieved at 330, 390, 630, 720 and 810 min successively; at 40 °C, those were 330, 390, 450, 630 and 720 min; at 60 °C, those were 180, 225, 390, 540 and 630 min.

As shown in Fig. 9, the equilibrium adsorption capacity of ASG onto the CA/OMMT_{60%} composites was affected by temperature. It increased with the increased temperatures from 20 to 60 °C. This indicated that the adsorption of ASG onto the surface of the CA/

OMMT_{60%} composites was favorable at enhanced temperatures, suggesting that such adsorption was an endothermic process. This was partly due to the fact that swelling behavior in the inner structure of CA/OMMT adsorbents was favorable at high temperatures. As such, it was conducive to the intake of dye molecules into adsorbents [45]. Before and after the equilibrium was reached, the adsorption capacity showed different trends at different temperatures. Generally, before the equilibrium was reached, the increase in the temperature led to an increase of adsorption rate, which indicated a thermodynamically controlled process.

3.7. Kinetics of adsorption

The kinetics of adsorption is one of the most important characteristics in defining the efficiency and application of an adsorptive material. Many studies suggested that the Lagergren's first-order (LFO) equation was suited for explaining liquid–solid adsorption kinetics and it was called the pseudo-first-order (PFO) equation [46]. So far the often-used kinetic models are the PFO equation and the pseudo-second-order equation (PSO) [47,48]. The pseudo-first-order kinetic equation can be expressed as:

$$q_t = q_1 \exp(1 - \exp(-k_1 t))$$

where q_1 and q_t are the amounts of the dye adsorbed at equilibrium and at time t (mg g^{-1}); k_1 is the pseudo-first-order rate constant (min^{-1}). When this model was applied to the adsorption of ASG, parameters q_1 and k_1 were obtained by using a non-linear least square method and the results are listed in Table 1. Pseudo-first order plots for the adsorption of ASG onto CA/OMMT_{60%} at various temperatures are given in Fig. 10, in which the solid lines represent the pseudo-first order model while the symbols represent the experimental data.

Here the applicability of the pseudo-first order model to the kinetic data of adsorption of ASG onto CA/OMMT_{60%} was compared with the pseudo-second order model. The pseudo-second-order kinetic model has the mathematical form as below:

$$q_t = q_2 \left(\frac{q_2 k_2 t}{1 + q_2 k_2 t} \right)$$

where q_2 is the maximum adsorption capacity (mg g^{-1}) and k_2 is the equilibrium rate constant of the pseudo-second-order adsorption ($\text{g mg}^{-1} \text{min}^{-1}$). Values of k_2 and q_2 were obtained by using a non-linear regression method. Fig. 11 depicts the pseudo-second order plots for the adsorption of ASG onto CA/OMMT_{60%} at various temperatures and the results are summarized in Table 1.

Both of the models seemed to be able to represent the kinetic data as illustrated in Table 1, Figs. 10 and 11. The correlation coef-

ficients for both models were greater than 0.95. However, to decide whether the model could well represent the experimental data or not, the physical meaning of each parameter involved in the model should be considered, rather than only based on the correlation coefficient. The k_1 parameter in the pseudo-first order model as well as the parameter k_2 in pseudo-second order are the time-scale factors. These parameters decide how fast the equilibrium condition in the system can be reached [49]. As the time-scale factors, usually both of the parameters are strongly dependent on the initial concentration of the adsorbate. The values of these parameters decrease with the increase of the initial concentration of the adsorbate. As indicated in Table 1, here both of parameters k_1 and k_2 obtained from the non-linear fitting decreased as the initial solution concentration of ASG increased. Nevertheless, just as mentioned above, the parameters q_1 and q_2 represent the amount of the adsorbate ASG adsorbed at the equilibrium condition. Usually the value of these parameters should be equal to those experimental values, which can be determined from the measurements of the equilibrium adsorption isotherms. As listed in Table 1, comparatively, the fitting values of the parameter q_1 in the Lagergren's first-order equation better represented the adsorption of ASG onto the composite and they were much closer to the experimental value. The results indicated that the pseudo-first order model was more suited for the adsorption of ASG onto CA/OMMT composites than the pseudo-second order model.

3.8. Adsorption isotherms and thermodynamic parameters

The adsorption isotherms were measured on the basis of the presumption of the Langmuir model and Freundlich model, respectively [50]. Theoretically, the Langmuir adsorption isotherm assumes that adsorption takes place at specific homogenous sites on the surface of the adsorbents and it is suited for the monolayer adsorption. The linear form of the Langmuir isotherm equation can be expressed as below:

$$\frac{1}{q_e} = \frac{1}{q_{\max}} + \left(\frac{1}{q_{\max} K_L} \right) \frac{1}{C_e} \quad (2)$$

where q_e is the equilibrium dye concentration on the adsorbent (mol g^{-1}), C_e the equilibrium dye concentration in the solution (mol dm^{-3}), q_{\max} the monolayer adsorption capacity of the adsorbent (mol g^{-1}) and K_L is the Langmuir adsorption constant ($\text{dm}^3 \text{mol}^{-1}$) related to the free energy of adsorption. The plots of $1/q_e$ versus $1/C_e$ for the adsorption of ASG onto the CA/OMMT_{60%} composites were made to generate the slope of $1/(q_{\max} K_L)$ and intercept $1/q_{\max}$ (Fig. 12a).

Table 1
Kinetic parameters for the adsorption of ASG on CA/OMMT_{60%}.

T (°C)	C_0 (mg dm^{-3})	q_e (exp) (mg g^{-1})	k_1 (min^{-1})	q_1 (mg g^{-1})	r_1^2	k_2 ($\times 10^{-4}$) ($\text{g mg}^{-1} \text{min}^{-1}$)	q_2 (mg g^{-1})	r_2^2
20	25	47.5	0.022	47.4	0.995	5.935	51.8	0.998
	50	89.3	0.017	88.7	0.994	2.419	98.1	0.999
	75	121.7	0.011	115.9	0.943	1.185	130.5	0.998
	100	135.3	0.008	131.5	0.985	0.581	154.9	0.996
	125	164.7	0.012	161.3	0.996	0.771	184.8	0.999
40	25	48.9	0.039	48.2	0.989	11.21	51.6	0.992
	50	93.7	0.017	92.3	0.989	2.186	102.4	0.995
	75	128.0	0.017	124.3	0.981	1.706	137.1	0.993
	100	139.2	0.012	135.0	0.981	1.004	152.9	0.995
	125	177.3	0.010	172.7	0.992	0.603	199.7	0.994
60	25	49.2	0.038	49.3	0.993	10.58	52.7	0.996
	50	95.6	0.026	95.8	0.992	3.661	103.7	0.987
	75	131.3	0.024	126.8	0.930	2.540	137.6	0.987
	100	152.1	0.017	147.1	0.985	1.404	163.7	0.998
	125	193.0	0.015	188.4	0.989	0.941	210.8	0.987

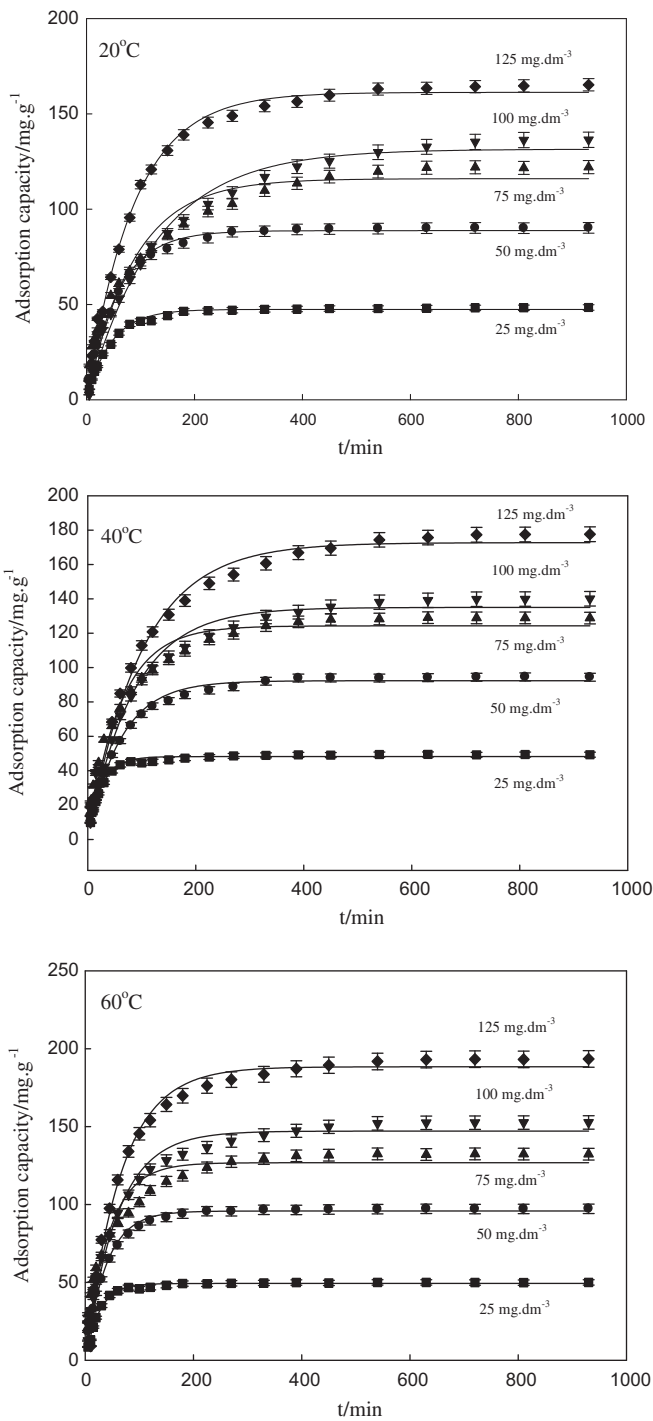


Fig. 10. Pseudo-first-order kinetic plots for the adsorption of ASG onto CA/OMMT-60% at temperature: (a) 20 °C, (b) 40 °C, and (c) 60 °C.

The Freundlich isotherm is an empirical equation which is usually used to describe heterogeneous systems. A linear form of the Freundlich equation is

$$\ln q_e = \ln K_F + 1/n \ln C_e$$

where K_F ($\text{dm}^3 \text{g}^{-1}$) and n are constants for a given adsorbate (ASG) and adsorbent (CA/OMMT_{60%}). The constants are indicative of the extent of the adsorption and the degree of non-linearity between the concentration of the solution and the adsorbed amount, respectively. From the plots of $\ln q_e$ versus $\ln C_e$ for the adsorption of ASG

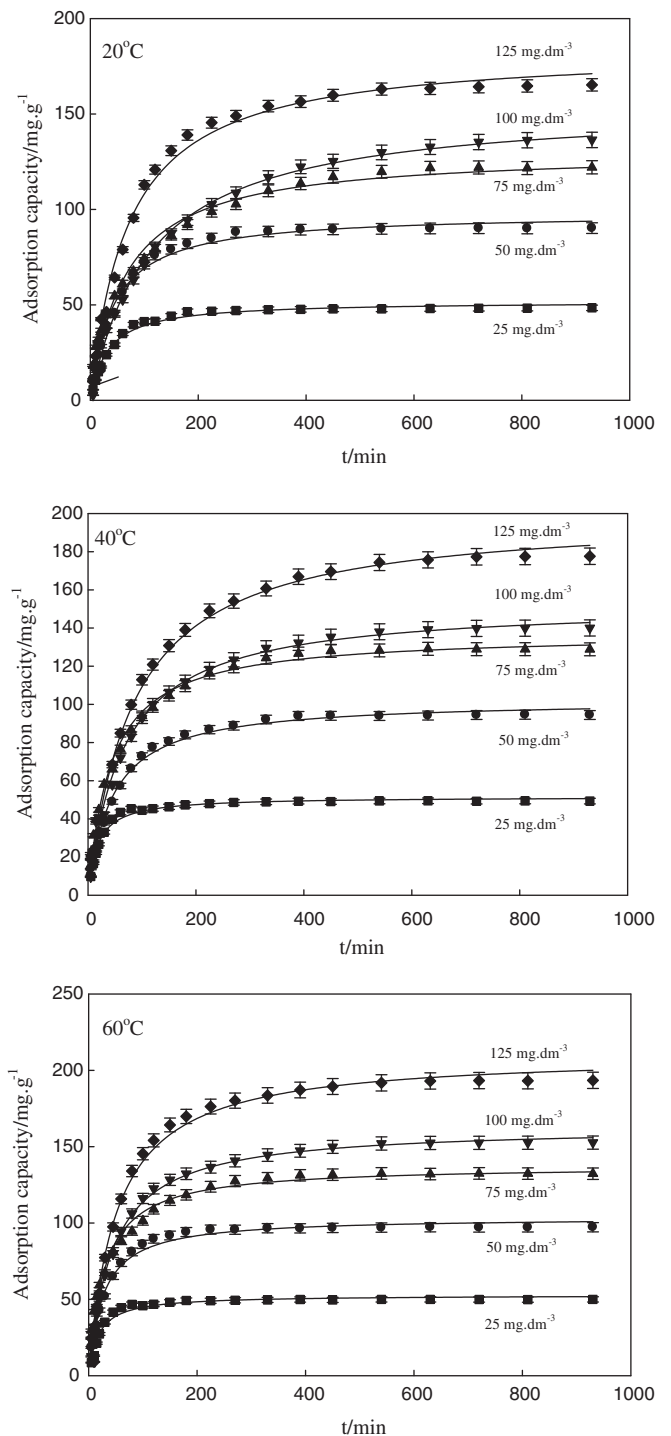


Fig. 11. Pseudo-second-order kinetic plots for the adsorption of ASG onto CA/OMMT-60% at various temperatures: (a) 20 °C, (b) 40 °C and (c) 60 °C.

onto the CA/OMMT_{60%} composites (Fig. 12b), the intercept value of K_F and the slope of $1/n$ were obtained.

The parameters from Langmuir and Freundlich models for the adsorption of ASG are listed in Table 2. When the r^2 values are compared, the Langmuir model correlation coefficients are in a range of 0.96–0.98, while the Freundlich model correlation coefficients are between 0.95 and 0.98. Hence, the isotherms fit into Langmuir models a bit better. In other words, the adsorption process of the CA/OMMT_{60%} composites tends to be a homogeneous adsorption on the surface. In addition, the essential feature of the

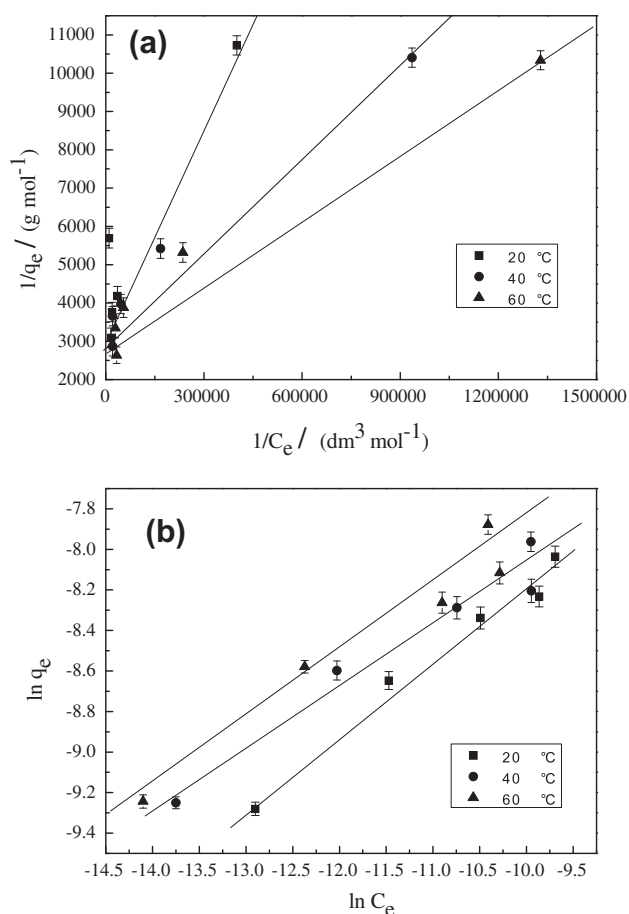


Fig. 12. (a) Langmuir plots and (b) Freundlich plots for the adsorption of ARG onto CA/OMMT_{60%} at various temperatures.

Langmuir isotherm can be reflected by 'R_L', which is a dimensionless constant and is referred to as a separation factor or an equilibrium parameter. R_L is calculated using the following equation:

$$R_L = \frac{1}{1 + K_L C_0}$$

where K_L is the Langmuir constant (dm³ mol⁻¹) and C₀ is the initial dye concentration (mol dm⁻³). The values of R_L calculated based on such an equation are listed in Table 2.

Equilibrium constant K_L varies with the temperature. It can be used to estimate thermodynamic parameters, such as the changes in the standard free energy (G°), enthalpy (H°) and entropy (S°) associated to the adsorption process. These values were determined by using following equations and the data are given in Table 3.

$$\Delta G^\circ = -RT \ln K_L$$

$$\ln K_L = -\frac{\Delta G^\circ}{RT} = -\frac{\Delta H^\circ}{RT} + \frac{\Delta S^\circ}{R}$$

The overall standard free energy change during the adsorption process was between -29.5 and -36.9 kJ mol⁻¹, suggesting that

Table 2
Langmuir and Freundlich isotherm constants for the adsorption of ASG onto CA/OMMT-60% at various temperatures.

T (°C)	Langmuir				Freundlich		
	q _{max} (×10 ⁻⁴) (mol g ⁻¹)	K _L (×10 ⁵) (dm ³ mol ⁻¹)	r _L ²	R _L (×10 ⁻³)	K _F (×10 ⁻³) (dm ³ g ⁻¹)	n	r _F ²
20	2.965	1.813	0.983	21.967	10.467	2.757	0.981
40	2.881	4.629	0.970	8.726	6.266	3.331	0.957
60	3.041	6.090	0.964	6.642	8.951	3.189	0.953

Table 3
Thermodynamic parameters calculated from the Langmuir isotherm data for the adsorption of ASG onto the CA/OMMT_{60%}.

T (K)	ΔG° (kJ mol ⁻¹)	ΔH° (kJ mol ⁻¹)	ΔS° (J k ⁻¹ mol ⁻¹)
293	-29.5	24.8	186.2
313	-34.0		
333	-36.9		

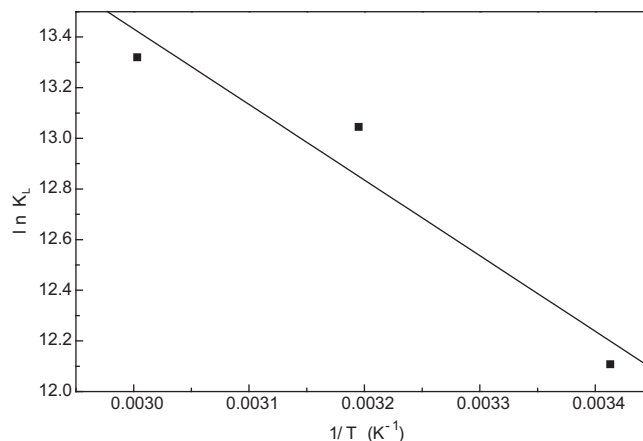


Fig. 13. Plot of ln K_L to 1/T for calculation of thermodynamic parameters.

the process included both physical and chemical adsorption. As for the adsorption of ASG onto the CA/OMMT_{60%} composites, the plot of ln K_L as a function of 1/T (Fig. 13) gave a straight line. The H° and S° were calculated from the slope and intercept of the plot, respectively (Table 3). The positive value of the standard enthalpy change (24.8 kJ mol⁻¹) clearly indicated that the adsorption of ASG onto the CA/OMMT_{60%} composites was a spontaneous and endothermic process. It was reasonable in consideration of the hydrophobicity of OMMT and the macroporosity of the composites.

4. Conclusion

The preparation and shaping of the inorganic–organic composites from cellulose acetate molecules and organo-montmorillonite platelets led to a new class of paper-like materials. In particular, the resultant materials can act as functional adsorbents for the adsorption of the organic pollutants in the wastewater, with the merits in the aspects of easy operation and separation. For the fabrication of such composites, OMMT first needed to be produced through the ion exchange of cetyltrimethyl ammonium cations with Na⁺ cations in the interlayer space of pristine montmorillonite, followed by the dispersion of CA and OMMT in acetone. Then the mixture underwent a self-assembly process through gradual evaporation of acetone, leading to the formation of the paper-like composites of cellulose acetate and organo-montmorillonite.

The characterization of composites by XRD, FTIR, SEM, and TG analyses indicated that there existed several interactions among CA molecules and OMMT platelets. These included cross-linking reactions between OMMT platelets and CA chains, intermolecu-

larly and intramolecularly; aggregations of clay platelets and intercalation of part of CA in the interlayers of OMMT. Dependent on the ratio of CA to OMMT, a dense or macroporous paper-like composites can be created.

The macroporous paper-like CA/OMMT composites showed a remarkable capacity for the adsorption of Acid Scarlet G anionic dye from aqueous solution. The OMMT components played a dominant role in the adsorption. As such, when the content of OMMT in the CA/OMMT composites was increased from 10 wt.% to 60 wt.%, the adsorption capacities of ASG onto CA/OMMT increased from 3.1 mg g⁻¹ to 85.7 mg g⁻¹, respectively, under the present experimental conditions. The pH value of the dye solution, adsorption temperature, and the initial dye concentration had effects on the amount of the adsorption of ASG onto CA/OMMT and the time to reach adsorption equilibrium. A series of measurements on ASG onto the CA/OMMT_{60%} composites suggested that the adsorption kinetics of ASG on such CA/OMMT composites obeyed the Lagergren's pseudo-first-order model. The adsorption of ASG onto the CA/OMMT_{60%} composites was a spontaneous and endothermic process and the adsorption isotherm of ASG could be depicted by the Langmuir equation. Noticeably, such paper-like composites from natural minerals and bioresources are environmentally benign. As demonstrated in this work, they possess adsorption capacity of organic species with advantages of easy operation and separation. All these allow them to find many promising applications in future.

Acknowledgements

The authors wish to acknowledge the financial support from the Distinguished Young Scholar Grants from the Natural Scientific Foundation of Zhejiang Province (R4100436), the Natural Scientific Foundation of Zhejiang Province (LQ12B03004), the National Natural Scientific Foundation of China (20773110, 20541002), Zhejiang "151" talents project, and International Collaborative Project (2009C14G2020021) from the Science and Technology Department of Zhejiang Provincial Government for the related research and development. CHZ proposed the research, designed composites and wrote the paper. DZ conducted the experiments, and provided the data and drafted the article. Other authors contributed to providing technical or scientific assistance during this work.

References

- G.F. Jiang, C.H. Zhou, X. Xia, F.Q. Yang, D.S. Tong, W.H. Yu, S.M. Liu, Controllable preparation of graphitic carbon nitride nanosheets via confined interlayer nanospace of layered clays, *Mater. Lett.* 64 (2010) 2718–2721.
- H.S. Xia, C.H. Zhou, D.S. Tong, W.H. Yu, S.M. Liu, Preparation and catalysis in epoxidation of allyl chloride of zeolitic titanasilicate-1/smectitic clay minerals, *Appl. Clay Sci.* 53 (2011) 279–287.
- H.H. Murray, Traditional and new applications for kaolin, smectite, and palygorskite: a general overview, *Appl. Clay Sci.* 17 (2000) 207–221.
- C.H. Zhou, Emerging trends and challenges in synthetic clay-based materials and layered double hydroxides, *Appl. Clay Sci.* 48 (2010) 1–4.
- D. Zhang, C.H. Zhou, C.X. Lin, D.S. Tong, W.H. Yu, Synthesis of clay minerals, *Appl. Clay Sci.* 50 (2010) 1–11.
- C.H. Zhou, Z.F. Shen, L.H. Liu, S.M. Liu, Preparation and functionality of clay-containing films, *J. Mater. Chem.* 21 (2011) 15132–15153.
- C.H. Zhou, An overview on strategies towards clay-based designer catalysts for green and sustainable catalysis, *Appl. Clay Sci.* 53 (2011) 97–105.
- B.S. Krishna, D.S.R. Murty, B.S. Jai Prakash, Surfactant-modified clay as adsorbent for chromate, *Appl. Clay Sci.* 20 (2001) 65–71.
- K.G. Bhattacharyya, S.S. Gupta, Adsorption of a few heavy metals on natural and modified kaolinite and montmorillonite: a review, *Adv. Colloid Interface Sci.* 140 (2008) 114–131.
- W. Shen, H.P. He, J.X. Zhu, P. Yuan, R.L. Frost, Grafting of montmorillonite with different functional silanes via two different reaction systems, *J. Colloid Interface Sci.* 313 (2007) 268–273.
- S.A. Boyd, M.M. Mortland, C.T. Chiou, Sorption characteristic of organic compounds on hexadecyltrimethylammonium-smectite, *Soil Sci. Soc. Am. J.* 52 (1988) 652–657.
- J.H. Bae, D.I. Song, Y.W. Jeon, Adsorption of anionic dye and surfactant from water onto organomontmorillonite, *Sep. Sci. Technol.* 35 (2000) 353–365.
- F. Lopez Arbeloa, M.J. Tapia Estevez, T. Lopez Arbeloa, I. Lopez Arbeloa, Spectroscopic study of the adsorption of rhodamine 6G on clay minerals in aqueous suspensions, *Clay Miner.* 32 (1997) 97–106.
- N. Miyamoto, R. Kawai, K. Kuroda, M. Ogawa, Adsorption and aggregation of a cationic cyanine dye on layered clay minerals, *Appl. Clay Sci.* 16 (2000) 161–170.
- A.H. Gemeay, Adsorption characteristics and the kinetics of the cation exchange of Rhodamine-6G with Na⁺-montmorillonite, *J. Colloid Interface Sci.* 251 (2002) 235–241.
- X.N. Wang, N.W. Zhu, B.K. Yin, Preparation of sludge-based activated carbon and its application in dye wastewater treatment, *J. Hazardous Mater.* 153 (2008) 22–27.
- J.K. Xie, Q.Y. Yue, B.Y. Gao, Q. Li, Adsorption kinetics and thermodynamics of anionic dyes onto sewage sludge derived activated carbon, *Int. J. Environ. Pollut.* 45 (2011) 123–144.
- H. Shao, S. Shao, H.B. Wang, H. Cheng, Experimental study on the treatment of acid scarlet wastewater with modified bentonite, *Sci. Technol. Rev.* 27 (2009) 89–92.
- H.Y. Zhu, J. Ru, Preparation of cross-linked chitosan film and its absorption behavior of acid scarlet dyeing, *J. Hebei Univ. Sci. Technol.* 30 (2009) 54–57.
- M.N. Mohammad, N. Farhood, Synthesis, amine functionalization and dye removal ability of titania/silica nano-hybrid, *Microporous Mesoporous Mater.* 156 (2012) 153–160.
- D.S. Tong, C.H. Zhou, Y. Lu, H.Y. Yu, G.F. Zhang, W.H. Yu, Adsorption of acid red G dye on octadecyl trimethylammonium montmorillonite, *Appl. Clay Sci.* 50 (2010) 427–431.
- H.M. Park, A.K. Mohanty, L.T. Drzal, E. Lee, D.F. Mielewski, M. Misra, Effect of sequential mixing and compounding conditions on cellulose acetate/layered silicate nanocomposites, *J. Polym. Environ.* 14 (2006) 27–35.
- L.A. White, Preparation and thermal analysis of cotton-clay nanocomposites, *J. Appl. Polym. Sci.* 92 (2004) 2125–2131.
- S.S. Ray, M. Bousmina, Biodegradable polymers and their layered silicate nanocomposites: in greening the 21st century materials world, *Prog. Mater. Sci.* 50 (2005) 962–1079.
- C.H. Zhou, X. Xia, C.X. Lin, D.S. Tong, J. Beltrami, Catalytic conversion of lignocellulosic biomass to fine chemicals and fuels, *Chem. Soc. Rev.* 40 (2011) 5588–5617.
- R. Morita, F.Z. Khan, T. Sakaguchi, M. Shiotsuki, Y. Nishio, T. Masuda, Synthesis, characterization, and gas permeation properties of the silyl derivatives of cellulose acetate, *J. Membr. Sci.* 305 (2007) 136–145.
- X.Y. Wang, Y.M. Du, J.W. Luo, Chitosan/organic rectorite nanocomposite films: Structure, characteristic and drug delivery behaviour, *Carbohydr. Polym.* 69 (2007) 41–49.
- R.B. Romero, C.A.P. Leite, M.D.C. Goncalves, The effect of the solvent on the morphology of cellulose acetate/montmorillonite nanocomposites, *Polymer* 50 (2009) 161–170.
- H. Fischer, Polymer nanocomposites: from fundamental research to specific applications, *Mater. Sci. Eng. C* 23 (2003) 763–772.
- B.J. Pan, W.M. Zhang, L. Lv, Q.X. Zhang, S.R. Zheng, Development of polymeric and polymer-based hybrid adsorbents for pollutants removal from waters, *Chem. Eng. J.* 151 (2009) 19–29.
- C.H. Zhou, D.S. Tong, M.H. Bao, Z.X. Du, Z.H. Ge, X.N. Li, Generation and characterization of catalytic nanocomposite materials of highly isolated iron nanoparticles dispersed in clays, *Top. Catal.* 39 (2006) 213–219.
- R. Liu, R.L. Frost, W.N. Martens, Near infrared and mid infrared investigations of adsorbed phenol on HDTMAB organoclays, *Mater. Chem. Phys.* 113 (2009) 707–713.
- Q. Zhou, R.L. Frost, H. He, Y. Xi, H. Liu, Adsorbed para-nitrophenol on HDTMAB-A TEM and Infrared spectroscopic study, *J. Colloid Interface Sci.* 307 (2007) 357–363.
- K.H.S. Kung, K.F. Hayes, Fourier-transform infrared spectroscopic study of the adsorption of cetyltrimethylammonium bromide and cetylpyridinium chloride on silica, *Langmuir* 9 (1993) 263–267.
- S.W. Jang, J.C. Kim, J.H. Chang, Preparation and characterization of cellulose nanocomposite films with two different organo-micas, *Cellulose* 16 (2009) 445–454.
- C. Danumah, M. Bousmina, S. Kaliaguine, Novel polymer nanocomposites from templated mesostructured inorganic materials, *Macromolecules* 36 (2003) 8208–8209.
- S. Tunc, O. Duman, Preparation and characterization of biodegradable methyl cellulose/montmorillonite nanocomposite films, *Appl. Clay Sci.* 48 (2010) 414–424.
- M. Alexandre, P. Dubois, Polymer-layered silicate nanocomposites: preparation, properties and uses of a new class of materials, *Mater. Sci. Eng. Res.* 28 (2000) 1–63.
- W. Xie, R. Xie, W.P. Pan, D. Hunter, B. Koene, L.S. Tan, R. Vaia, Thermal stability of quaternary phosphonium modified montmorillonites, *Chem. Mater.* 14 (2002) 4837–4845.
- D.S. Tong, C.H. Zhou, Catalytic hydrolysis of cellulose to reducing sugar over acid-activated montmorillonite catalysts, *Appl. Clay Sci.*, in press.
- M.D.C. Lucena, A.E.V. de Alencar, S.E. Mazzeto, S.D. Soares, The effect of additives on the thermal degradation of cellulose acetate, *Polym. Degrad. Stab.* 80 (2003) 149–155.

- [42] E. Biçer, C. Arat, A voltammetric study on the aqueous electrochemistry of acid red 1 (azophloxine), *Croat. Chem. Acta* 82 (2009) 583–593.
- [43] A.S. Ozcan, B. Erdem, A. Ozcan, Adsorption of acid blue 193 from aqueous solutions onto Na-bentonite and DTMA-bentonite, *J. Colloid Interface Sci.* 280 (2004) 44–54.
- [44] Z. Wu, I.S. Ahn, C.H. Lee, J.H. Kim, Y.G. Shul, K.T. Lee, Enhancing the organic dye adsorption on porous xerogels, *Colloids Surf. A: Physicochem. Eng. Asp.* 240 (2004) 157–164.
- [45] K.G. Bhattacharyya, A. Sarma, Adsorption characteristics of the dye, brilliant green, on neem leaf powder, *Dyes Pigm.* 57 (2003) 211–222.
- [46] R.L. Tseng, F.-C. Wu, R.-S. Juang, Characteristics and applications of the Lagergren's first-order equation for adsorption kinetics, *J. Taiwan Inst. Chem. Eng.* 41 (2010) 661–669.
- [47] Y.S. Ho, G. McKay, Sorption of dye from aqueous solution by peat, *Chem. Eng. J.* 70 (1998) 115–124.
- [48] A. Ozcan, E.M. Oncu, A.S. Ozcan, Kinetics, isotherm and thermodynamic studies of adsorption of Acid Blue 193 from aqueous solutions onto natural sepiolite, *Colloid. Surf. A* 277 (2006) 90–97.
- [49] W. Plazinski, W. Rudzinski, A. Plazinska, Theoretical models of sorption kinetics including a surface reaction mechanism: a review, *Adv. Colloid Interface Sci.* 152 (2009) 2–13.
- [50] A.S. Ozcan, B. Erdem, A. Ozcan, Adsorption of acid blue 193 from aqueous solutions onto BTMA-bentonite, *Colloid Surf. A: Physicochem. Eng. Asp.* 266 (2005) 73–81.